

# Is the present expansion of the universe really accelerating?

R G Vishwakarma

Inter-University Centre for Astronomy and Astrophysics (IUCAA),  
 Post Bag 4, Ganeshkhind, Pune 411 007, India  
 Email: vishwa@iucaa.ernet.in

## Abstract

The current observations are usually explained by an accelerating expansion of the present universe. However, with the present quality of the supernovae Ia data, the allowed parameter space is wide enough to accommodate the decelerating models as well. This is shown by considering a particular example of the dark energy equation of state  $w_\phi \equiv p_\phi/\rho_\phi = -1/3$ , which is equivalent to modifying the *geometrical curvature* index  $k$  of the standard cosmology by shifting it to  $(k - \alpha)$  where  $\alpha$  is a constant. The resulting decelerating model is consistent with the recent CMB observations made by WMAP, as well as, with the high redshift supernovae Ia data including SN 1997ff at  $z \approx 1.7$ .

**Key words:** cosmology: theory, CMB observations, SN Ia observations, dark energy.

## 1 INTRODUCTION

It is generally believed that the expansion of the present universe is accelerating, fuelled by some hypothetical source with negative pressure collectively known as '*dark energy*'. This belief is mainly motivated by the high redshift supernovae (SN) Ia observations, which cannot be explained by the decelerating Einstein deSitter model which used to be the favoured model before these observations were made a few years ago. (It may, however, be noted that if one takes into account the absorption of light by the intergalactic metallic dust which extinguishes radiation travelling over long distances, then the observed faintness of the extragalactic SN Ia can be explained successfully in the framework of the Einstein deSitter model. This issue will be discussed in a later section. In the rest of the discussion, we shall not include this effect.)

Although the best-fitting standard model to the SN Ia data predicts an accelerating expansion, however, it should be noted that the low density

open models, which predict a decelerating expansion, also fit the SN Ia observations reasonably well. Unfortunately, these models are ruled out by the recent measurements of the angular power fluctuations of CMB including the first year observations made by WMAP.

In this paper we show, by considering a particular example, that both these observations (and many others too) can still be explained by a decelerating model of the universe in the mainstream cosmology.

The observed SN Ia explosions look fainter than their luminosity in the Einstein-deSitter model. This observed faintness is explained by invoking a positive cosmological constant  $\Lambda$  following the fact that the luminosity distance of an object can be increased by incorporating a ‘*matter*’ with negative pressure in Einstein’s equations. However, a constant  $\Lambda$ , is plagued with the so called the cosmological constant problem: Why don’t we see the large vacuum energy density  $\rho_v \equiv \Lambda/8\pi G = \rho_{\text{Pl}} \approx 10^{76} \text{ GeV}^4$ , expected from particle physics which is  $\approx 10^{123}$  times larger than the value required by the SN observations? Or, why are the radiation energy density and the energy density in  $\Lambda$  ( $\Lambda/8\pi G$ ) set to an accuracy of better than one part in  $10^{123}$  at the Planck time in order to ensure that the densities in matter and  $\Lambda$  become comparable at precisely the present epoch? (Padmanabhan 2002; Peebles & Ratra 2002; Sahni & Starobinsky 2000). A phenomenological solution to understand the smallness of  $\Lambda$  is supplied by a dynamically decaying  $\Lambda$ . A popular candidate is an evolving large-scale scalar field  $\phi$ , commonly known as *quintessence*, which does not interact with matter ( $T_{\phi}^{ij}_{;\,j} = 0$ ) and can produce negative pressure for a potential energy-dominated field (Peebles & Ratra 2002). This is equivalent to generalizing the equation of state of vacuum to

$$p_\phi = w_\phi \rho_\phi. \quad (1)$$

Moreover, it is always possible to add a term like  $T_{\phi}^{ij}$  on the right hand side of Einstein’s field equations independent of the geometry of the universe. The equation-of-state parameter  $w_\phi$  is, in general, some function of time and leads to a constant  $\Lambda$  for  $w_\phi = -1$ .

It would be worthwhile to mention here that there is another approach to solve the cosmological constant problem by invoking some phenomenological models of kinematical  $\Lambda$  which result either from some symmetry principle (Vishwakarma 2001a, 2001b), or from dimensional analysis (Vishwakarma 2000, 2002a; Carvalho, Lima & Waga 1992; Chen & Wu 1990) or just by

assuming  $\Lambda$  as a function of the cosmic time  $t$  or the scale factor  $S(t)$  of the R-W metric (for a list of this type of models, see Overduin & Cooperstock 1998). Although the quintessence fields also behave like a dynamical  $\Lambda$  (with  $\Lambda_{\text{effective}} \equiv 8\pi G\rho_\phi$ ), they are in general fundamentally different from the kinematical  $\Lambda$  models. In the former case, quintessence and matter fields are assumed to be conserved separately, whereas in the latter case, the conserved quantity is  $[T_{ij} + \{\Lambda(t)/8\pi G\}g_{ij}]$ . This characteristic of the kinematical  $\Lambda$  models makes them consistent with Mach's principle (Vishwakarma 2002b). However, in the following, we shall keep ourselves limited to the former case with a constant  $w_\phi$ .

## 2 FIELD EQUATIONS AND DISTANCE MEASURES

In order to study the constraints on the parameters coming from the different observations, we shall describe the model briefly in the following. For the R-W metric, the Einstein field equations, taken together with conservation of the energy, yield

$$H^2(z) = H_0^2 \left[ \Omega_{m0} (1+z)^3 + \Omega_{r0} (1+z)^4 + \Omega_{\phi0} (1+z)^{3(1+w_\phi)} - \Omega_{k0} (1+z)^2 \right], \quad (2)$$

$$q(z) = \frac{H_0^2}{H^2(z)} \left[ \frac{\Omega_{m0}}{2} (1+z)^3 + \Omega_{r0} (1+z)^4 + \frac{(1+3w_\phi)}{2} \Omega_{\phi0} (1+z)^{3(1+w_\phi)} \right], \quad (3)$$

where  $\Omega_i$  are, as usual, the different energy density components in units of the critical density  $\rho_c \equiv 3H^2/8\pi G$ :

$$\Omega_m \equiv \frac{8\pi G}{3H^2} \rho_m, \quad \Omega_r \equiv \frac{8\pi G}{3H^2} \rho_r, \quad \Omega_\phi \equiv \frac{8\pi G}{3H^2} \rho_\phi, \quad \Omega_k \equiv \frac{k}{S^2 H^2} \quad (4)$$

and the subscript 0 denotes the value of the quantity at the present epoch. Equation (2) at  $z = 0$  implies that  $\Omega_{m0} + \Omega_{r0} + \Omega_{\phi0} = 1 + \Omega_{k0}$ , by the use of which Equation (2) reduces to

$$\begin{aligned} H^2(z) = & H_0^2 \left[ \Omega_{m0} (1+z)^3 + \Omega_{r0} (1+z)^4 + \Omega_{\phi0} (1+z)^{3(1+w_\phi)} \right. \\ & \left. + (1 - \Omega_{m0} - \Omega_{r0} - \Omega_{\phi0}) (1+z)^2 \right]. \end{aligned} \quad (5)$$

In a homogeneous and isotropic universe, the different distance measures of a light source of redshift  $z$  located at a radial coordinate distance  $r_1$  are given by the following.

The *luminosity distance*  $d_L$ :

$$d_L = (1 + z)S_0 r_1, \quad (6)$$

The *angular diameter distance*  $d_A$ :

$$d_A = \frac{S_0 r_1}{(1 + z)}, \quad (7)$$

where  $r_1$  is given by

$$\frac{1}{S_0} \int_0^z \frac{dz'}{H(z')} = \begin{cases} \sin^{-1} r_1, & \text{when } k = 1 \\ r_1, & \text{when } k = 0 \\ \sinh^{-1} r_1, & \text{when } k = -1. \end{cases} \quad (8)$$

The present value of the scale factor  $S_0$ , appearing in equations (6 - 8) which measures the curvature of spacetime, can be calculated from equation (4) as

$$S_0 = H_0^{-1} \sqrt{\frac{k}{(\Omega_{m0} + \Omega_{r0} + \Omega_{\phi0} - 1)}}. \quad (9)$$

### 3 DEGENERACIES IN FRIEDMANN MODELS COMING FROM SN Ia OBSERVATIONS

Let us start with the SN Ia observations which directly measure the apparent magnitude  $m$  and the redshift  $z$  of the supernovae. The theoretically predicted (apparent) magnitude  $m(z)$  of a light source at a given redshift  $z$  is given in terms of its absolute luminosity  $M$  and the luminosity distance  $d_L$  through the relation

$$m(z) = \log_{10}[\mathcal{D}_L(z)] + \mathcal{M}, \quad (10)$$

where  $\mathcal{D}_L \equiv H_0 d_L$  is the dimensionless luminosity distance and  $\mathcal{M} \equiv M - 5 \log_{10} H_0 + \text{constant}$  (the value of the *constant* depends on the chosen units in which  $d_L$  and  $H_0$  are measured. For example, if  $d_L$  is measured in Mpc and  $H_0$  in  $\text{km s}^{-1} \text{Mpc}^{-1}$ , then this *constant* comes out as  $\approx 25$ ).

We consider the data on the redshift and magnitude of a sample of 54 SN Ia as considered by Perlmutter et al (excluding 6 outliers from the full sample of 60 SN) (Perlmutter et al 1999), together with SN 1997ff at  $z = 1.755$  ( $m^{\text{eff}} = 26.02 \pm 0.34$ ), the highest redshift supernova observed so far (Riess et al 1998, Narciso et al 2002).

The  $\chi^2$  value is calculated from its usual definition

$$\chi^2 = \sum_{i=1}^{55} \left[ \frac{m_i^{\text{eff}} - m(z_i)}{\delta m_i^{\text{eff}}} \right]^2, \quad (11)$$

where  $m_i^{\text{eff}}$  refers to the effective magnitude of the  $i$ th SN which has been corrected for the SN lightcurve width-luminosity relation, galactic extinction and K-correction and the dispersion  $\delta m_i^{\text{eff}}$  is the uncertainty in  $m_i^{\text{eff}}$ .

If one minimizes  $\chi^2$  in the standard cosmology ( $w_\phi = -1$ ) by varying the free parameters  $\Omega_{\text{m}0}$ ,  $\Omega_{\phi0} = \Omega_{\Lambda0}$  and  $\mathcal{M}$  (the contribution from the term containing  $\Omega_{\text{r}0}$  is negligible for this dataset and can be safely neglected), one finds that the best-fitting solution is  $\Omega_{\text{m}0} = 0.67$ ,  $\Omega_{\Lambda0} = 1.24$  and  $\mathcal{M} = 23.92$  with  $\chi^2 = 56.93$  at 52 degrees of freedom (dof) (= number of data points – number of fitted parameters), i.e.,  $\chi^2/\text{dof} = 56.93/52 = 1.09$ , a good fit indeed. A ‘rule of thumb’ for a *moderately* good fit is that  $\chi^2$  should be roughly equal to the number of dof. A more quantitative measure for the *goodness-of-fit* is given by the  $\chi^2$ -*probability* which is very often met with in the literature and its compliment is usually known as the *significance level* (should not be confused with the confidence regions). If the fitted model provides a typical value of  $\chi^2$  as  $x$  at  $n$  dof, this probability is given by

$$Q(x, n) = \frac{1}{\Gamma(n/2)} \int_{x/2}^{\infty} e^{-u} u^{n/2-1} du. \quad (12)$$

Roughly speaking, it measures the probability that *the model does describe the data and any discrepancies are mere fluctuations which could have arisen by chance*. To be more precise,  $Q(x, n)$  gives the probability that a model which does fit the data at  $n$  dof, would give a value of  $\chi^2$  as large or larger than  $x$ . If  $Q$  is very small, the apparent discrepancies are unlikely to be chance fluctuations and the model is ruled out.

The probability  $Q$  for the best-fitting standard model comes out as 29.7%, which represents a good fit. This model represents an accelerating expansion of the present universe according to equation (3), which suggests that the

present expansion will be accelerating if  $\Omega_{\phi 0} > \Omega_{m0}/2$ . Thus the best-fitting flat model ( $\Omega_m + \Omega_\Lambda = 1$ ) is also an accelerating one, which is obtained as  $\Omega_{m0} = 1 - \Omega_{\Lambda 0} = 0.31$  with  $\chi^2/\text{dof}=58.97/53=1.11$  and  $Q = 26.6\%$ .

Let us now examine the status of the decelerating models, particularly, the models with  $\Omega_\phi = 0$ . An important model in this category is the canonical Einstein-deSitter model ( $\Omega_{m0} = 1$ ,  $\Omega_{\Lambda 0} = 0$ ), which has a poor fit:  $\chi^2/\text{dof}=93.01/54 = 1.72$  with  $Q = 0.1\%$  and is ruled out. However, the open models with low  $\Omega_{m0}$  have reasonable fits. For example, the following decelerating models with  $\Lambda = 0$ ,

$$\Omega_{m0} = 0.2: \chi^2/\text{dof}=66.74/54 = 1.24, Q = 11.4\%;$$

$$\Omega_{m0} = 0.3: \chi^2/\text{dof}=68.78/54 = 1.27, Q = 8.5\%;$$

$$\Omega_{m0} = 0.4: \chi^2/\text{dof}=71.31/54 = 1.32, Q = 5.7\%, \text{etc.},$$

have reasonable fittings and by no means are rejectable. Open decelerating models with non-zero  $\Lambda$  ( $0 < \Omega_{\Lambda 0} < \Omega_{m0}/2$ ) have even better fit. The best-fitting model with a vanishing  $\Lambda$  is obtained as  $\Omega_{m0} = 0$  with  $\chi^2 = 64.6$  at 54 dof ( $\chi^2/\text{dof}= 1.2$ ) and  $Q = 15.3\%$ . Figure 1 shows the allowed regions by the data in the  $\Omega_{m0} - \mathcal{M}$  plane at different confidence levels for a vanishing  $\Lambda$  cosmology. Thus the low  $\Omega_{m0}$  open models with a vanishing  $\Lambda$  are fully consistent with the current SN Ia observations. Additionally, a low  $\Omega_{m0}$  is also consistent with the recent 2DF and Sloan surveys which give  $\Omega_{m0} = 0.23 \pm 0.09$  (Hawkins et al. 2002) and  $\Omega_{m0} \approx 0.14^{+0.11}_{-0.06}$  (at  $2\sigma$ ) (Dodelson et al. 2001). However, these models do not seem consistent with the first observations of the temperature angular power spectrum of the CMB measured by NASA's explorer mission "Wilkinson Microwave Anisotropy Probe" (WMAP) (Bennett et al., 2003), which are also consistent with the earlier observations (de Bernardis et al. 2000, 2002; Lee et al. 2001; Halverson et al. 2002; Siever et al. 2002). These observations, when fitted to the standard cosmology, appear to indicate that  $\Omega_{m0} + \Omega_{\Lambda 0} \approx 1$ .

## 4 THE PROPOSED MODEL

### 4.1 Motivation

We shall now consider a particular model of dark energy specified by the equation of state  $w_\phi = -1/3$ , which, as we shall show in the following, explains both the observations - SN Ia, as well as, CMB very well. The equation of state  $w_\phi = -1/3$ , for which  $\rho_\phi$  varies as  $1/S^2$  (say,  $\Omega_\phi = \alpha/S^2 H^2$ ),

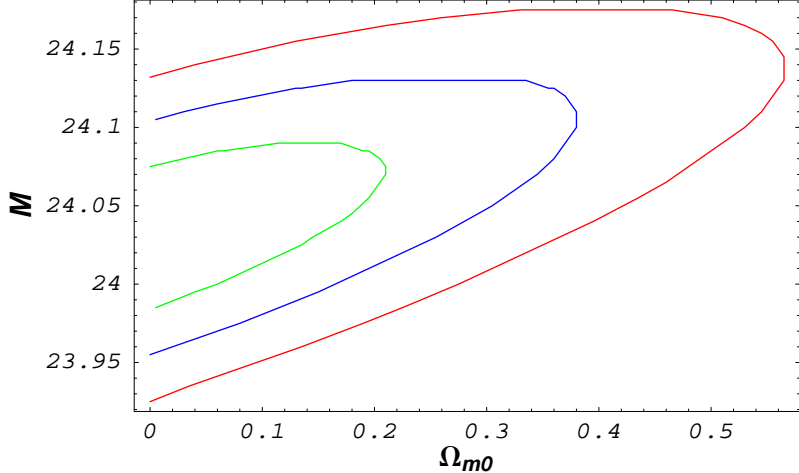


Figure 1: The allowed regions by the SN Ia observations are shown in the  $\Omega_{m0} - \mathcal{M}$  plane for  $\Omega_\phi = 0$  cosmology ( $\mathcal{M}$  is usually termed as the ‘*Hubble constant-free absolute luminosity*’). The ellipses, in the order of increasing size, correspond to respectively 68%, 95% and 99% confidence levels.

is interesting in its own right. For this case, the Hubble and the deceleration parameters yield

$$H^2(z) = H_0^2 \left[ \Omega_{m0} (1+z)^3 + \Omega_{r0} (1+z)^4 + (1 - \Omega_{m0} - \Omega_{r0}) (1+z)^2 \right], \quad (13)$$

$$q(z) = \frac{H_0^2}{H^2(z)} \left[ \frac{\Omega_{m0}}{2} (1+z)^3 + \Omega_{r0} (1+z)^4 \right], \quad (14)$$

which describe a decelerating expansion. Interestingly in this case,  $\Omega_{\text{matter}}$  ( $\equiv \Omega_m + \Omega_r$ ) alone is sufficient to describe  $H(z)$  completely, which gives the expansion dynamics of the universe. The additional knowledge of  $\Omega_{\phi 0}$  decides the curvature through  $\Omega_{k0} = \Omega_{m0} + \Omega_{r0} + \Omega_{\phi 0} - 1$ . Expressions (13) and (14) are the same as the ones in the standard cosmology with  $\Lambda = 0$ , with only one exception: in the standard cosmology,  $\Omega_{m0} + \Omega_{r0} = 1 + \Omega_{k0}$ , where as in the present model,  $\Omega_{m0} + \Omega_{r0} + \Omega_{\phi 0} = 1 + \Omega_{k0}$ . As mentioned earlier,  $\Omega_{\phi 0}$

contributes to the curvature through  $S_0 = H_0^{-1} \sqrt{k/(\Omega_{m0} + \Omega_{r0} + \Omega_{\phi0} - 1)}$  and hence to the different distance measures for  $k = \pm 1$  cases (for  $k = 0$ , distances do not depend on  $S_0$ ). Although  $\Omega_{\phi0}$  does not contribute to the expansion dynamics of the model (and neither to the distances for  $k = 0$  case), it helps  $\Omega_{m0}$  to assume even those values which are not allowed in the standard cosmology, and hence gives more leverage to  $\Omega_{m0}$ . It is in fact this property of the model which is instrumental in explaining the CMB observations even for low  $\Omega_{m0}$ , as we shall see in the following.

It may be noted that although the topological defects, like cosmic strings and textures also have an equation of state  $\rho + 3p = 0$  (i.e., their density falls off as  $1/S^2$ ), however, the converse of this is not true and a dark energy with  $w_\phi = -1/3$  need not necessarily be represented by cosmic strings. Moreover, this ‘pseudo-source’ term does not explicitly contribute to the expansion dynamics (and hence to the deceleration or to the expansion age) of the model but essentially to the curvature, as we have mentioned earlier. One can obtain the same cosmology by removing this term and simultaneously modifying the curvature index  $k$  by  $(k - \alpha)$  (Vishwakarma & Singh 2002). It would, therefore, be more appropriate to consider it as a shift in the *geometrical curvature* of the standard cosmology and not as a source term. This term also appears in the context of brane cosmology by adding a surface term of brane curvature scalar in the action (Vishwakarma & Singh 2002; Singh, Vishwakarma & Dadhich 2002).

## 4.2 CMB Observations

The temperature fluctuations  $\Delta T$  in the angular power spectra of the CMB correspond to oscillations in the  $\Delta T - \ell$  (Legendre multipole) space. The peaks of these oscillations can be explained in terms of the angle  $\theta_A$  subtended by the sound horizon at the last scattering epoch when CMB photons decoupled from baryons at  $z_{\text{dec}} = 1100$  (Hu & Dodelson 2002). The power spectrum of CMB can be characterized by the positions of the peaks and ratios of the peak amplitudes. It has long been recognized that the locations and amplitudes of the peaks in the region  $90 < \ell < 900$  (where the anisotropies are related to causal processes occurring in the photon-baryon plasma until recombination) are very sensitive to the variations in the parameters of the model and hence serve as a sensitive probe to constrain the cosmological parameters and discriminate among various models (Hu et al. 2001; Doran & Lilley 2001, 2002). In fact, for  $\ell > 40$ , the ratios of the peak

amplitudes are insensitive to the intrinsic amplitude of the CMB spectrum. This renders the positions of the peaks, particularly the position of the first peak, as a powerful probe of the parameters of the model. The first observations of WMAP have measured the position of the first peak very accurately at  $\ell = 220.1 \pm 0.8$  ( $1\sigma$ ) (Page et al. 2003), which we shall use in our fit.

The angle  $\theta_A$ , which is given by the ratio of sound horizon to the distance (*angular diameter distance*) of the last scattering surface, sets the acoustic scale  $\ell_A$  through

$$\ell_A = \frac{\pi}{\theta_A} = \frac{\pi (1 + z_{\text{dec}}) d_A(z_{\text{dec}})}{\int_{z_{\text{dec}}}^{\infty} c_s(z) dz / H(z)}, \quad (15)$$

where the speed of sound  $c_s$  in the plasma is given by  $c_s = 1/\sqrt{3(1+R)}$  and  $R \equiv 3\rho_b/4\rho_\gamma = 3\Omega_{b0}/[4\Omega_{\gamma0}(1+z)]$  corresponds to the ratio of baryon density to photon density. The location of  $i$ -th peak in the angular power spectrum is given by

$$\ell_{\text{peak}_i} = \ell_A(i - \delta_i), \quad (16)$$

where the phase shift  $\delta_i$ , caused by the plasma driving effect is determined predominantly by the pre-recombination physics (Hu et al. 2001) and can be approximated by

$$\delta_i = a_i \left\{ \frac{r(z_{\text{dec}})}{0.3} \right\}^{0.1}, \quad (17)$$

where  $a_i$  is respectively 0.267, 0.24 and 0.35 for  $\text{peak}_1$ ,  $\text{peak}_2$  and  $\text{peak}_3$  and  $r(z_{\text{dec}}) \equiv \rho_r(z_{\text{dec}})/\rho_m(z_{\text{dec}}) = \Omega_{r0}(1+z_{\text{dec}})/\Omega_{m0}$  is the ratio of radiation and matter energy densities at the decoupling era.

Let us recall that  $\Omega_{r0}$  gets contributions from photons (CMB) as well as from neutrinos, i.e.,  $\Omega_r = \Omega_\gamma + \Omega_\nu$ . The present photon contribution to the radiation can be estimated by the CMB temperature  $T_0 = 2.728\text{K}$ . This gives  $\Omega_{\gamma0} \approx 2.48 h^{-2} \times 10^{-5}$ , where  $h$  is the present value of the Hubble parameter in units of  $100 \text{ km s}^{-1} \text{ Mpc}^{-1}$ . The neutrino contribution follows from the assumption of 3 neutrino species, a standard thermal history and a negligible mass compared to its temperature (Hu & Dodelson 2002). This gives  $\Omega_{\nu0} \approx 1.7 h^{-2} \times 10^{-5}$ . When these values are used in equations (15)-(17), they produce  $\ell_{\text{peak}_i}$  in the observed range for sufficiently big ranges of the free parameters  $\Omega_{m0}$ ,  $\Omega_{\phi0}$ ,  $\Omega_{b0}$  and  $h$ . For example, for  $\Omega_{b0} = 0.05$  and  $h = 0.65$ , the following choices of  $\Omega_{m0}$  and  $\Omega_{\phi0}$  yield:

$$\Omega_{m0} = 0.3, \Omega_{\phi0} = 0.6 \rightarrow \ell_{\text{peak}_1} = 222.5, \ell_{\text{peak}_2} = 536.7, \ell_{\text{peak}_3} = 808.2;$$

$$\Omega_{m0} = 0.25, \Omega_{\phi0} = 0.65 \rightarrow \ell_{\text{peak}_1} = 225.0, \ell_{\text{peak}_2} = 545.1, \ell_{\text{peak}_3} = 820.9;$$

$$\Omega_{m0} = 0.2, \Omega_{\phi0} = 0.72 \rightarrow \ell_{\text{peak}_1} = 220.0, \ell_{\text{peak}_2} = 540.7, \ell_{\text{peak}_3} = 814.3,$$

which are in good agreement with  $\ell_{\text{peak}_1} = 220.1 \pm 0.8$  and  $\ell_{\text{peak}_2} = 546 \pm 10$  measured by WMAP. These measurements are also consistent with other observations, for example, the BOOMERANG project (de Bernardis et al., 2002) measured the first three peaks in the ranges:

$\ell_{\text{peak}_1} : 200 - 223, \ell_{\text{peak}_2} : 509 - 561, \ell_{\text{peak}_3} : 820 - 857$  at 68% confidence level; and

$\ell_{\text{peak}_1} : 183 - 223, \ell_{\text{peak}_2} : 445 - 578, \ell_{\text{peak}_3} : 750 - 879$  at 95% confidence level. These ranges are also in agreement with many other observations like, MAXIMA, DASI, CBI, etc., at least on the location of the first peak (Lee et al. 2001; Halverson et al. 2002; Sievers et al. 2002).

In Figure 2, we have shown the allowed region in the  $\Omega_{m0} - \Omega_{\phi0}$  plane which produces the first peak  $\ell_{\text{peak}_1} = 220.1 \pm 0.8$  (68% confidence level). For this purpose, we varied  $\Omega_{b0}$  in the range  $0 - 0.1$  and  $h$  in the range  $0.5 - 0.8$  and marginalized over these parameters to obtain the allowed ranges of  $\Omega_{m0}$  and  $\Omega_{\phi0}$ .

### 4.3 SN Ia Observations

For the SN Ia data in the present model,  $\chi^2$  decreases for lower values of  $\Omega_{m0}$  and gives the minimum  $\chi^2$  for negative  $\Omega_{m0}$ . For example, for the flat model, the minimum value of  $\chi^2$  is obtained as 62.93 for  $\Omega_{m0} = -0.31 = 1 - \Omega_{\phi0}$  and  $\mathcal{M} =$  at 53 dof, which is though not physical. A ‘physically viable’ best-fitting solution, in this case, can be regarded as  $\Omega_{m0} = 0$ , which gives  $\chi^2/\text{dof} = 64.56/53 = 1.22$  for  $\Omega_{\phi0} = 0.14$  and  $\mathcal{M} = 24.03$  with  $Q = 13.3\%$ . This represents a reasonably good fit, though not as good as the best fit in the standard cosmology with a constant  $\Lambda$ . The allowed region by the data is sufficiently large, as shown in Figure 2, and low density models, consistent with CMB, are easily accommodated within the 95% confidence region (Note that the allowed region by the CMB is shown only at  $1\sigma$  level. At higher levels, the region will be wider). For example, the following models represent reasonable fit.

$$\Omega_{m0} = 0.3, \Omega_{\phi0} = 0.6: \chi^2/\text{dof} = 71.93/54 = 1.33 \text{ with } Q = 5.18\%;$$

$$\Omega_{m0} = 0.25 = 1 - \Omega_{\phi0}: \chi^2/\text{dof} = 71.36/54 = 1.32 \text{ with } Q = 5.69\%;$$

$$\Omega_{m0} = 0.25, \Omega_{\phi0} = 0.65: \chi^2/\text{dof} = 70.76/54 = 1.31 \text{ with } Q = 6.26\%;$$

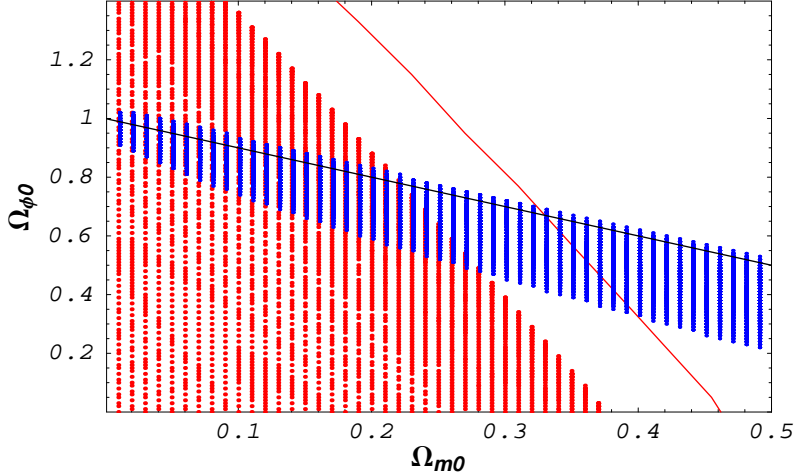


Figure 2: The blue region shows the allowed ranges of  $\Omega_{m0}$  and  $\Omega_{\phi 0}$  by the CMB at 68% confidence level (to produce the first peak in the range  $220.1 \pm 0.8$ ). This has been obtained after marginalizing over  $\Omega_{b0}$  and  $h$  (where  $H_0 = 100h \text{ km s}^{-1} \text{ Mpc}^{-1}$ ). Here we have varied  $h$  in the range  $0.5 - 0.8$  and  $\Omega_{b0}$  in the range  $0 - 0.1$ . The red-shaded contour corresponds to 95% confidence region from the SN Ia data (marginalized over  $\mathcal{M}$ ) and the red curve corresponds to the boundary of the 99% confidence region given by the same data (in calculating these regions, the extinction of SN light by metallic whiskers, as discussed in section 5, has not been taken into account). The line in black corresponds to the flat model  $\Omega_{m0} + \Omega_{\phi 0} = 1$ .

$\Omega_{m0} = 0.2$ ,  $\Omega_{\phi 0} = 0.7$ :  $\chi^2/\text{dof} = 69.63/54 = 1.29$  with  $Q = 7.46\%$ , etc.  
 One can go up to even as high as  $\Omega_{m0} = 0.4$  at 99% confidence level.

#### 4.4 Age of the Universe

The parameters  $H_0$  and  $\Omega_{m0}$  set the age of the universe in this model. Remember that there is still a big uncertainty in the present value of  $H_0$ . Sandage and his collaborators find  $H_0 = 58 \pm 6 \text{ km s}^{-1} \text{ Mpc}^{-1}$  from an analysis of SN Ia distances (Parodi et al. 2000). This is also consistent with the value obtained from an analysis of clusters using Sunyaev-Zeldovich effect which gives  $H_0 = 60 \pm 10 \text{ km s}^{-1} \text{ Mpc}^{-1}$  (Birkinshaw 1999). A Hubble

Space Telescope Key Project supplies  $H_0 = 64^{+8}_{-6} \text{ km s}^{-1} \text{ Mpc}^{-1}$  (Saurabh et al. 1999). Some experiments also measure higher  $H_0$ , for example, by using the fluctuations in the surface brightness of galaxies as distance measure, it has been found that  $H_0 = 74 \pm 4 \text{ km s}^{-1} \text{ Mpc}^{-1}$  (Blakeslee et al. 1999). Thus it appears that  $H_0$  lies somewhere in the range  $(58 - 74) \text{ km s}^{-1} \text{ Mpc}^{-1}$ . An average value of  $H_0 = 65 \text{ km s}^{-1} \text{ Mpc}^{-1}$  from this range, constrains  $\Omega_{m0}$  of the model by  $0 < \Omega_{m0} \leq 0.34$  to give  $t_0 \geq 12 \text{ Gyr}$ , so that the age of the oldest objects detected so far, e.g., the globular clusters of age  $t_{\text{GC}} = 12.5 \pm 1.2 \text{ Gyr}$  (Cayrel et al. 2001; Gnedin et al. 2001) can be explained. The presently favoured value  $\Omega_{m0} \approx 0.25$  easily accommodates in this range.

## 5 EXTINCTION BY METALLIC DUST

In this section, we shall discuss an issue related with SN Ia observations which is generally avoided by most of the authors while discussing  $m - z$  relation for SNe Ia. This is the absorption of light by metallic dust. The intergalactic dust is claimed to be dominated by whiskers which form from the condensation of the metallic vapours ejected from the supernovae explosions. Such whiskers are subsequently pushed out of the galaxy through pressure of shock waves (Hoyle & Wickramasinghe, 1988; Narlikar et al, 1997). Experiments have shown that metallic vapours on cooling, condense into elongated whiskers of  $\approx 0.5 - 1 \text{ mm}$  length and  $\approx 10^{-6} \text{ cm}$  cross-sectional radius (Hoyle et al, 2000). Indeed this type of dust extinguishes radiation travelling over long distances (Aguire, 1999; Vishwakarma, 2002a).

In an isotropic and homogeneous universe, the contribution to the effective magnitude arising from the absorption of light by the intervening whisker-like dust, is given by

$$\Delta m(z) = \int_0^{l(z)} \kappa \rho_g dl = \kappa \rho_{g0} \int_0^z (1+z')^2 \frac{dz'}{H(z')}, \quad (18)$$

where  $\kappa$  is the mass absorption coefficient, which is effectively constant over a wide range of wavelengths and is of the order  $10^5 \text{ cm}^2 \text{ g}^{-1}$  (Wickramasinghe & Wallis, 1996),  $\rho_g \propto S^{-3}$  is the whisker grain density with  $\rho_{g0}$  in the range  $(3 - 5) \times 10^{-34} \text{ g cm}^{-3}$  and  $l(z)$  is the proper distance traversed by light through the intergalactic medium emitted at the epoch of redshift  $z$ . The net magnitude is then given by

$$m^{\text{net}}(z) = m(z) + \Delta m(z), \quad (19)$$

where the first term on the r.h.s. corresponds to the usual magnitude from the cosmological evolution given by equation (10).

We note that taking account of this effect improves the fit to the SN Ia data considerably. For example, the model with  $\Omega_{m0} = 0.25$ ,  $\Omega_{\phi0} = 0.65$  now gives  $\chi^2/\text{dof} = 65.25/53 = 1.23$  with  $Q = 12.05\%$ . Even the Einstein-deSitter model ( $\Omega_{m0} = 1$ ,  $\Omega_{\phi0} = 0$ ) gives an acceptable fit:  $\chi^2/\text{dof} = 68.40/53 = 1.29$  with  $Q = 7.57\%$ . Interestingly, this model (Einstein-deSitter) is also consistent with the CMB observations:  $\Omega_{b0} = 0.05$  and  $h = 0.65$  yield  $\ell_{\text{peak}_1} = 202.9$ ,  $\ell_{\text{peak}_2} = 476.8$ ,  $\ell_{\text{peak}_3} = 717.6$ . One can improve the fit by increasing  $\Omega_{b0}$  and/or decreasing  $h$ . Also a better fit can be obtained in open models. For example, the model  $\Omega_{m0} = 0.87$ ,  $\Omega_{\phi0} = 0$  with  $\Omega_{b0} = 0.05$  and  $h = 0.65$  yields  $\ell_{\text{peak}_1} = 220.1$ ,  $\ell_{\text{peak}_2} = 518.8$ ,  $\ell_{\text{peak}_3} = 780.9$ . The fit to the SN Ia data (accounting the extinction by metallic whiskers) is also acceptable:  $\chi^2/\text{dof} = 67.89/53 = 1.28$  with  $Q = 8.18\%$ . However, these models suffer from the age problem if  $h$  is not sufficiently low. For example,  $h$  should be  $\leq 54$  for  $\Omega_{m0} = 1$  with  $\Omega_{\phi0} = 0$ .

## 6 CONCLUSION

There seems to be an impression in the community that the current observations, particularly the high redshift SN Ia observations and the measurements of the angular power fluctuations of the CMB, can be explained only in the framework of an accelerating universe. This, however, does not seem correct. The allowed parameter space by the datasets is wide enough to accommodate decelerating models also. We have shown that both these observations can also be explained in a decelerating low density-model with a dark energy equation of state  $w_{\phi} = -1/3$  and the preferred curvature of the spatial section is negative. For this equation of state, the resulting ‘dark energy’ does not contribute to the expansion dynamics of the model (described by the Hubble parameter) and contributes to the curvature only.

It may be noted that the case  $w_{\phi} = -1/3$  is not special in any sense to the datasets and slightly more decelerating or slightly accelerating models are also consistent with both the observations. In order to verify this, we change  $w_{\phi}$  slightly from  $w_{\phi} = -1/3$  (in both directions) to, say,  $w_{\phi} = -0.3$  and  $w_{\phi} = -0.35$  and check the status of the resulting models. The result is the following.

$w_\phi = -0.3$ :

A test model, for example,  $\Omega_{m0} = 0.25$ ,  $\Omega_{\phi0} = 0.65$ ,  $\Omega_{b0} = 0.05$  and  $h = 0.65$  yields  $\ell_{\text{peak}_1} = 220.2$ ,  $\ell_{\text{peak}_2} = 533.4$ ,  $\ell_{\text{peak}_3} = 803.2$  from the CMB and  $\chi^2/\text{dof} = 72.10/54 = 1.34$  with  $Q = 5.04\%$  from the SN Ia.

$w_\phi = -0.35$ :

The same test model yields  $\ell_{\text{peak}_1} = 227.3$ ,  $\ell_{\text{peak}_2} = 550.5$ ,  $\ell_{\text{peak}_3} = 829.1$  from the CMB and  $\chi^2/\text{dof} = 70.12/54 = 1.3$  with  $Q = 6.92\%$  from the SN Ia. These fits are acceptable and comparable to their respective values for  $w_\phi = -1/3$  mentioned in sections 4.2 and 4.3.

We also note that if we take into account the extinction of supernova light by the inter-galactic metallic dust, then the high redshift SN Ia data can also be explained by the models without any dark energy, such as, the Einstein-deSitter model. These models are also consistent with CMB observations. In fact, there is a degeneracy in the  $\Omega_{m0} - \Omega_{\phi0}$  plane along a line  $\Omega_{m0} + \Omega_{\phi0} \approx 1$  and a wide range of  $\Omega_{m0}$  is consistent with the CMB data.

We conclude that it is premature to claim, on the basis of the existing data, that the present expansion of the universe is accelerating (or decelerating). Only more accurate SN Ia data can remove this ambiguity, as  $q$  is sensitive significantly to the SN Ia data only. CMB observations are consistent with both - accelerating as well as decelerating models, as mentioned above. This endeavour may be accomplished by the proposed *SuperNova Acceleration Probe* (SNAP) experiment which aims to give accurate luminosity distances of type Ia supernovae up to  $z \approx 1.7$ .

## ACKNOWLEDGEMENTS

The author thanks DAE for his Homi Bhabha postdoctoral fellowship and T. Padmanabhan for useful comments and discussions.

## REFERENCES

- Aguire A. N., 1999, ApJ, 512, L19
- Bennett et al., astro-ph/0302207
- de Bernardis P., et al., 2002, ApJ., 564, 559
- Blakeslee J. P., et al., 1999, ApJ. Lett., 527, 73
- Birkinshaw M., 1999, Phys. Rep., 310, 97
- Cayrel R., et al, 2001, Nature, 409, 691
- Carvalho J. C., Lima J. A. S., Waga I., 1992, Phys. Rev. D, 46, 2404
- Chen W., Wu Y. S., 1990, Phys. Rev. D, 41, 695

Dodelson S., et al., astro-ph/0107421

Doran M., Lilley M., Schwindt J., Wetterich C., 2001, ApJ., 559, 501

Doran M., Lilley M., 2002, MNRAS, 330, 965

Gnedin O. Y., Lahav O., Rees M. J., astro-ph/0108034

Halverson N. W. et al., 2002, ApJ., 568, 38

Hawkins E., et al., astro-ph/0212375

Hoyle F., Wickramasinghe N. C., 1988, *Astrophys. Space Sc.* 147, 245

Hoyle F., Burbidge G., Narlikar J. V., 2000, *A Different Approach to Cosmology*, (Cambridge: Cambridge Univ. Press)

Hu W., Dodelson S., 2003, *Ann. Rev. Astron. Astrophys.*, 40, 171

Hu W., Fukugita M., Zaldarriaga M., Tegmark M., 2001, ApJ., 549, 669

Lee A. T. et al., 2001, ApJ., 561, L1

Narciso B., et al., 2002, ApJ., 577, L1 (astro-ph/0207097)

Narlikar J. V., Wickramasinghe N. C., Sachs R., Hoyle F., 1997, *Int. J. Mod. Phys. D*, 6, 125

Overduin J. M., Cooperstock F. I., 1998, *Phys. Rev. D*, 58, 043506

Padmanabhan T., hep-th/0212290

Page et al., astro-ph/0302220

Parodi B. R., et al., 2000, ApJ., 540, 634

Peebles P. J. E., Ratra B., astr0-ph/0207347

Perlmutter S., et al., 1999, ApJ., 517, 565

Riess A. G., et al., 2001, ApJ., 560, 49

Sahni V., Starobinsky A., 2000, *Int. J. Mod. Phys. D* 9, 373

Saurabh J., et al., 1999, ApJ. Suppl., 125, 73

Sievers J. L. et al., astro-ph/0205387

Singh P., Vishwakarma R. G., Dadhich N., hep-th/0206193

Vishwakarma R. G., 2000, *Class. Quantum Grav.*, 17, 3833

Vishwakarma R. G., 2001a, *Gen. Relativ. Grav.*, 33, 1973

Vishwakarma R. G., 2001b, *Class. Quantum Grav.* 18, 1159

Vishwakarma R. G., 2002a, MNRAS, 331, 776

Vishwakarma R. G., 2002b, *Class. Quantum Grav.* 19, 4747

Vishwakarma R. G., Singh P., astro-ph/0211285

Wickramasinghe N. C., Wallis D. H., 1996, *Astrophys. Space Sc.* 240, 157